Pitting growth detection in the gear transmission system of a locomotive using statistical features

Mohammad Ali Rezvani[1*], Farshad Niksai[2]

[1,2] School of Railway Engineering, Iran University of Science and Technology, Tehran, Iran

ARTICLE INFO	A B S T R A C T
	The reliability of power transmission systems in locomotives directly impacts the availability and safety of trains. The failure of gears, like pitting on teeth, is a common failure that can affect vehicle dynamics and reduce the safety and reliability of the system. Based on frequent visual inspections, detecting early-stage pitting is important to prevent more damage. The purpose of this research is to investigate the possibility of pitting detection in the early stage. For this purpose, the dynamic response of the gear system with pitting defects in different scenarios is evaluated and compared. The dynamic interaction between the gear system and other elements, such as the traction motor and wheelset, is regarded based on the operation condition. Also, the time-variant mesh stiffness is considered the primary internal excitation in the dynamics of the gear system. An analytical method based on the potential energy is used. The effect of pitting growth in different scenarios on the dynamic response in both time and frequency domains is studied. Some statistically representative features are computed for different scenarios. Features most sensitive to failure that enable the detection of gear tooth pitting and its propagation are introduced. The theoretical results are compared and validated with a laboratory test setup.

1. Introduction

Locomotives are complex machines with many critical components. Considering the wide usage of gears in power transmission systems shows that there would be great benefits. With a closer look, advantages like constant transmission ratio, high reliability, and high efficiency are specified [1]. The problem is the various gear faults that occur regarding depraved working conditions such as heavy loads and high fatigue [2]. The gear defect causes about 60% of gearbox failures [3]. The most materialized failures are tooth cracks, tooth surface pitting, and tooth breakage [3].

These failures of gears have been identified by maintenance experts in field operations. In the presence of failure, the vibrational performance of the vehicle detracts from normal operation. Failure occurrence causes discontinuity in the power transmission, and in more intense cases, it may lead to derailment or train disaster. This creates a drastic problem with the trustworthiness of the train operation. So, for the safety of train operation and optimizing the

maintenance cost, detecting failure in the early stages is of great importance.

Despite the explanations, the gear transmission system of locomotives and their dynamic performance have not been of prime importance to the researchers.

Besides, studying the faults in the power transmission gears of locomotives is rarely investigated. To recognize the fault, theoretical research is also needed. Fortunately, the dynamics of the gears and their time-varying mesh stiffness for a healthy and defective gear, based on vibration analysis, have attracted considerable attention.

Several reports focused on the vibrational motion of defective gears and suggested different models. These models varied in their degrees of freedom. The researchers discussed the simplest models with one degree of freedom and complex multi-degrees of freedom. Another important thing in modeling is how to model mesh stiffness [4-9]. The models are changed depending on the consideration of torsional motion or coupled with longitudinal motion [10-12]. Bartholomeus introduced a model with 8 degrees of freedom. Feng and Zhao [11] reported a planetary gearbox and proposed a mathematical model for inquiring about the pitting failure using frequency modulation and amplitudes; however, their model was unable to simulate the pitting progress. Moreover, the connection between the physical components of the gearbox and the model remained unnoticed. Chaari et al. [2], Zhe et al. [13], and Abu El-Seoud et al. [14] worked on pitting and modeled it as rectangular. Chari et al. [15] and Choi et al. [16] tried to correct the shape of the pit. Nevertheless, there is still no relationship between pitting growth and time-variant mesh stiffness in their study.

Many researchers used potential energy to specify the mesh stiffness and vibration displacement for faulty teeth [17-19].

Most studies have concentrated on the occurrence of just one failure on one tooth, although lately, limited research has modeled multiple faults on multiple teeth [20-22]. Rezaei et al. [23] studied detecting multi-cracks in helical gear teeth, making use of the transmission error ratio. Several pits on multiple teeth modeled in a circular shape have been simulated by Liang, and mesh stiffness is calculated by using potential energy [24]. Hou et al. considered the effect of pitting on mesh stiffness and vibration response [25]. Thunuguntla et al. used the finite element method to investigate the effect of pitting damage on a spur gear. [26]. Grzeszkowski classified pitting damage using vibration measurements [27].

Recently, some researchers considered multiple faults and coexisting damages on a gear [28-30]. Niksai and Rezvani modeled pitting and chipping faults concurrently [31]. Ouyang et al. diagnosed and analyzed pitting-crack coupling faults [32].

Considering the importance of the safety and accessibility of the locomotives, it is important to identify pitting propagation. Detecting pitting propagation is the main purpose of the present research. The simulation and determination of the amount of damage to the gear need to be as fast as possible. It would then result in higher dynamic efficiency. Pinion failure incurs a lot of costs, and the broken pinion can cause a lot of trouble, like derailment, and endanger the safety of railway transportation.

The present research also endeavors to uncover the earliest possible level at which the removed surface can be detected. Hence, the effect of pitting growth due to geometric parameters like the radius of pitting, number of pittings, and number of teeth with pits are examined.

For this purpose, a detailed theoretical dynamic model of the locomotive transmission system is built. This model considers torsional and longitudinal vibrations as well as the dynamic components' flexibility. Since this paper investigated the gear failures, the irregularities in the rail have been discarded. The input speed is considered constant. For calculating the time-varying mesh stiffness, the potential energy is used. Based on the calculated vibrational response, the statistical features indicate the failure, and the most relevant features are introduced. This is the best method for this aim [9] and may lead to better results in fault detection by providing useful information [33]. For this purpose, various indices, like statistical features, were proposed [34-36].

Furthermore, an experimental rig setup for a power transmission system with a 1/5 scale is constructed. This setup is then used for

validating the statistical parameter and determining the accuracy of the statistical parameter further.

It must be noted that the field observations provided in this study are mostly focused on the presence of multi-pitting on a single tooth and multiple teeth in a gear. This scheme, to the knowledge of the authors, has not been previously used for the fault detection of locomotive transmission systems. The statistical features provided in this study are further discussed in the results and discussion section. The variations in parametric studies were examined, and the ones with the highest sensitivity were applied in the experimental setup for validation.

2. Evaluating mesh stiffness and tooth pitting modeling

2.1. Tooth failure modeling

Pitting takes place on the teeth of the gears due to metal-to-metal contact. It can be visible in darker patches or shallow indentations on the toothed surfaces. These irregularities cause friction, resulting in lots of heat being generated. Pitting is a form of surface fatigue that may occur soon after the operation begins. Based on the visual inspection, it was found that pitting has the highest percentage among all types of gear failure. Pitting growth may lead to severe damage and a reduction in train safety.

Figure 1 displays a real pitting defect in the pinion of the power transmission system of a locomotive at an early stage. Identification of this failure before the critical level is very important for the safety and accessibility of locomotives. Theoretically, pitting cases are numerous, encompassing a wide range of defects, such as changes in the radius of each pit, the number of pits on each tooth, and the number of faulty teeth.

Fig. 1 Real pitting in the gear power transmission system of a locomotive.

Pitting can be reproduced in a different number of teeth. In this study, a more realistic mathematical modeling of pitting is considered. A variety of six defect cases are considered. The details for the different failure cases concerning the actual sizes of defects are as follows:

Table 1 Defect types and characteristics of one tooth.

Case No.	Number of pitted teeth	Number of pittings on each tooth	Removed surface (%)
1	1	1	0.5
2	3	1	1.5
3	6	1	3.1
4	1	6	3.1
5	3	6	9.4
6	6	6	18.8

Due to the geometry of the pits on the pinion's surface, the pit radius and depth are assumed to be 2 mm and 0.5 mm, respectively. The detection of these pittings is the main purpose of the simulation procedures. Determining the amount of damage on a gear as soon as possible would then result in longer gearbox life and higher dynamic proficiency.

2.2. Evaluating mesh stiffness

Many reports were interested in calculating mesh stiffness for pitting based solely on potential energy. Tian *et al.* computed mesh stiffness for chipping, and Liang *et al.* did the same for pitting [24,19]. They modeled the tooth as a cantilever beam. The entire cumulative energy in the meshing tooth pair included the Hertzian, bending, axial, and shear energies, corresponding to Hertzian, bending, axial, and shear stiffness.

The tooth profile is modeled with involute profiles, regarding the tooth profiles of the locomotive power transmission systems. Manufacturing and transmission errors are neglected. Lubrication is assumed to be ideal. The gear core is considered rigid, while the gear teeth are flexible. This procedure is also used in multiple research projects in this field.

Figure 2 represents a schematic of multiple pits on the tooth surface. To simplify the equation derivation, a straight line was used instead of the tooth fillet curve. The parameters (u, r, δ) specify the pitting on the tooth surface. The interval between the pit center and the root is u, the radius of the pit circle is r, and δ is the pitting depth. The compressive stiffness k_a, shear stiffness k_s, and bending stiffness k_b are only affected by pitting and are obtained as follows [37]:
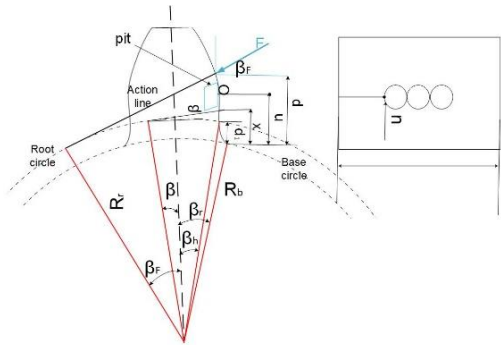

Fig. 2 Multiple pitting failure [34].

The values of Young's modulus and Poisson's ratio are represented with E and υ, and the width of the teeth with L. Z and N are the number of teeth and pits, respectively. F represents the pressure angle and is decomposed into its components with respect to β_F, which is the angle between the action line and the horizontal line. β_h and β_r, represent half of the tooth angle on the base circle and the root circle. ΔL_xj,

ΔI_xj, and ΔA_xj (generated by the jth pitting), correspondingly, demonstrate the reduction of the width of the tooth contact, the inertia of the tooth section and its area, and the interval to the contact point is x. The values of ΔL_xj, ΔI_xj, and ΔA_xj are calculated as follows:

$$
\frac{1}{k_b}
= \frac{[1 - \frac{(Z-2.5)\cos\beta_F \cos\beta_r}{Z\cos\beta_p}]^3 - (1-\cos\beta_F\cos\beta_h)^3}{2EL\cos\beta_F\sin^3\beta_h}
$$
$$
+ \int_{-\beta_F}^{\beta_h} \frac{3\{1+\cos\beta_F[(\beta_h-\beta)\sin\beta - \cos\beta]\}^2 (\beta_h-\beta)\cos\beta}{E(2L[\sin\beta + (\beta_h-\beta)\cos\beta]^3 - 3\sum_1^N \frac{\Delta I_{xj}}{R_b^3})} d_\beta
\tag{1}
$$

$$
\frac{1}{k_s}
= \frac{1.2(1+v)\cos^2\beta_F (\cos\beta_h - \frac{Z-2.5}{Z\cos\beta_p}\cos\beta_r)}{EL\sin\beta_h}
$$
$$
+ \int_{-\beta_F}^{\beta_h} \frac{1.2(1+v)(\beta_h-\beta)\cos\beta\cos^2\beta_F}{E(L[\sin\beta + (\beta_h-\beta)\cos\beta] - 0.5\sum_1^N \frac{\Delta A_{xj}}{R_b}} d_\beta
\tag{2}
$$

$$
\frac{1}{k_a}
= \frac{\sin^2\beta_F (\cos\beta_h - \frac{Z-2.5}{Z\cos\beta_p}\cos\beta_r)}{EL\sin\alpha_h}
$$
$$
+ \int_{-\beta_{F,i}}^{\beta_h} \frac{(\beta_h-\beta)\cos\beta \sin^2\beta_F}{E(2L[\sin\beta + (\beta_h-\beta)\cos\beta] - \sum_1^N \frac{\Delta A_{xj}}{R_b})} d_\beta
\tag{3}
$$

$$
\Delta L_x = \begin{cases} 2\sqrt{r^2 - (u-x)^2} & x \in [u-r, u+r] \\ 0 \end{cases}
\tag{4}
$$

$$
\Delta A_x = \begin{cases} \Delta L_x \delta & x \in [u-r, u+r] \\ 0 \end{cases}
\tag{5}
$$

$$
\Delta I_x = \begin{cases} \frac{1}{12}\Delta L_x \delta^3 + \frac{A_x \Delta A_x (h_x - \delta/2)^2}{A_x - \Delta A_x} \\ 0 \end{cases}
\tag{6}
$$
$$
x \in [u-r, u+r]
$$

According to Yang's research [38], the Hertz stiffness for a paired tooth is linearized to a constant value along the whole action line:

$$
k_h = \frac{\pi E(L_{eff})}{4(1-v^2)}
\tag{7}
$$

For pitting, L_{eff} is defined as follows [24]:

$$L_{eff} = \begin{cases} L, & otherwise \\ L - 2\sqrt{r^2 - (u - x)^2}, & u - r < x < u + r \end{cases} \quad (8)$$

One pair or two pairs of tooth contacts are happening in a pair of gears with a contact ratio between 1 and 2.

The equation for calculating the total mesh stiffness in a single-tooth-pair meshing interval is [37]:

$$K_t = \frac{1}{\frac{1}{k_h} + \frac{1}{k_{b1}} + \frac{1}{k_{s1}} + \frac{1}{k_{a1}} + \frac{1}{k_{b2}} + \frac{1}{k_{s2}} + \frac{1}{k_{a2}}} \quad (9)$$

$$k_t = k_{t_1} + k_{t_2} \quad (10)$$

$$= \sum_{i=1}^{2} \frac{1}{\frac{1}{k_{h,i}} + \frac{1}{k_{b1,i}} + \frac{1}{k_{s1,i}} + \frac{1}{k_{a1,i}} + \frac{1}{k_{b2,i}} + \frac{1}{k_{s2,i}} + \frac{1}{k_{a2,i}}} \quad (11)$$

The 1 and 2 indexes stand for the driving and driven gear, while index i represents the ith paired tooth.

3. Modeling of the power transmission system in a locomotive

3.1. Dynamic modeling

The power transmission system of a locomotive consists of a simple single-stage gearbox. For simulating torsional and longitudinal motions, an eight-degrees-of-freedom model is used. To have an accurate model, it is endeavored to simulate all the related components. For this purpose, the axle and the rotor are assumed to be flexible. Also, regarding the accurate model, the masses and moments of inertia of the gears of standard power transmission systems are computed using the SolidWorks engineering software. The specifications of the gear used in the locomotive power transmission system is presented in Table 2.

Table 2 Mechanical properties of the gears in the gearbox.

Characteristics	Pinion (driving)	Gear (driven)
Number of teeth	60	17
Module (mm)	11.3	11.3
Angle of attack	20	20
Mass (kg)	192	21
Face width (mm)	123	123
Young's modulus (GPa)	206	206
Poisson's ratio	0.3	0.3

The dynamic model is illustrated schematically in Fig. 3. T_m is the torque that drives the traction motor. The resistance torque is presented as T_w. The driver and driven shafts are assumed to be flexible. All components of the system are in good physical condition and without any installation problems. Lubrication conditions are also considered ideal. To focus on the impact of failures, the effect of rail irregularities is ignored.
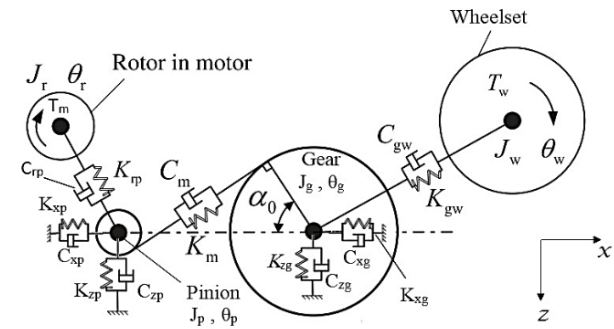

Fig. 1 Dynamic model of a power transmission system in a locomotive [4].

Regarding the additions to the model that are provided in this research, including the flexibility of the input and output drive shafts, the dynamic equations are elucidated in [30].

3.2. Numerical analysis

In order to evaluate the system specifics based on the above-given sets of equations, a numerical analysis must be performed. Therefore, it is required to simulate the displacement signals of the pinion.

Amabili and Rivola [39] reported that the proportion of gear mesh damping to gear mesh stiffness is constant and is about 0.07. The locomotive speed is assumed to be constant at 60 km/h. The angular velocity and torque are computed based on the specified velocity.

The traction motor provided 6 KNm of torque on the rotor, and the torque according to the gear ratio is 1.7 KNm. The pinion speed is 18.7 Hz, and the meshing gear frequency is 317.9 Hz. For calculations, the ode-15s solver with a frequency of 1 MHz from MATLAB software is used.

4. Results and discussion

4.1. Reduction in mesh stiffness

As explained earlier, six different cases are defined to represent the different pitting levels. With the use of the equations that were described in Section 2.2, the mesh stiffness of the paired teeth in the six designated cases is evaluated.

With the fault growth, it can be seen that the mesh stiffness is reduced during the tooth engagement period. Furthermore, the reduction in mesh stiffness is quantified using Eq. (11).

The differences in mesh stiffness of the healthy and faulty gear at the same angular displacement are calculated using Eq. (12). The results are presented in Table 3.

$$\delta_{k_t} = \left(\left| \sum_{f=1}^{F} \frac{k_{t1s}}{F} - \sum_{h=1}^{H} \frac{k_{t2m}}{H} \right| / \sum_{h=1}^{H} \frac{k_{t2m}}{H} \right) * 100\% \quad (12)$$

**Table 3** Averaged mesh stiffness reduction (%) caused by tooth.

Mesh period No.	Single-tooth-pair meshing duration					
	Case 1	Case 2	Case 3	Case 4	Case 5	Case 6
1	0.49	0.49	0.49	6.26	6.26	6.26
2	0	0.48	0.48	0	6.02	6.02
3	0	0.47	0.47	0	5.99	5.99
4	0	0	0.47	0	0	5.96
5	0	0	0.47	0	0	5.91
6	0	0	0.46	0	0	5.84
	Double-tooth-pair meshing duration					
1	0.01	0.01	0.01	0.13	0.13	0.13
2	0	0	0.01	0.05	0	0.05
3	0	0	0.01	0.05	0	0.05
4	0	0	0.01	0	0	0.06
5	0	0	0.01	0	0	0.06
6	0	0	0.01	0	0	0.07

In Eq. (12), k_{t1} stands for the mesh stiffness of a faulty gear, and k_{t2} represents the mesh stiffness of a perfect gear. F and H, respectively, represent the calculated mesh stiffness for defective gear and healthy gear.

4.2. Vibrational response

Figure 4 demonstrates the calculated vibrational signal for the six pre-defined scenarios. The results are for two complete pinion rotations with a period of 0.1 seconds.

Considering the 17 teeth for the pinion, in one complete revolution, 17 contacts occur. For two full-pinion revolutions, 34 peaks are present. In a healthy gear, the amplitude of the peaks is the same due to the teeth being in the same conditions. The study continues with calculating the vibrational behavior of the pinion for the defective cases. Obviously, for the defective pinions, the amplitude of vibrations due to contacts does not stay the same and will behave variably depending on the conditions of the contacts.
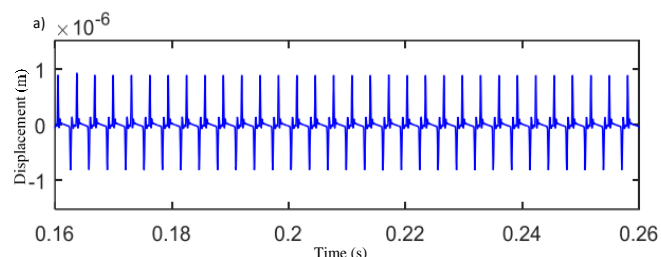
a) Case 1
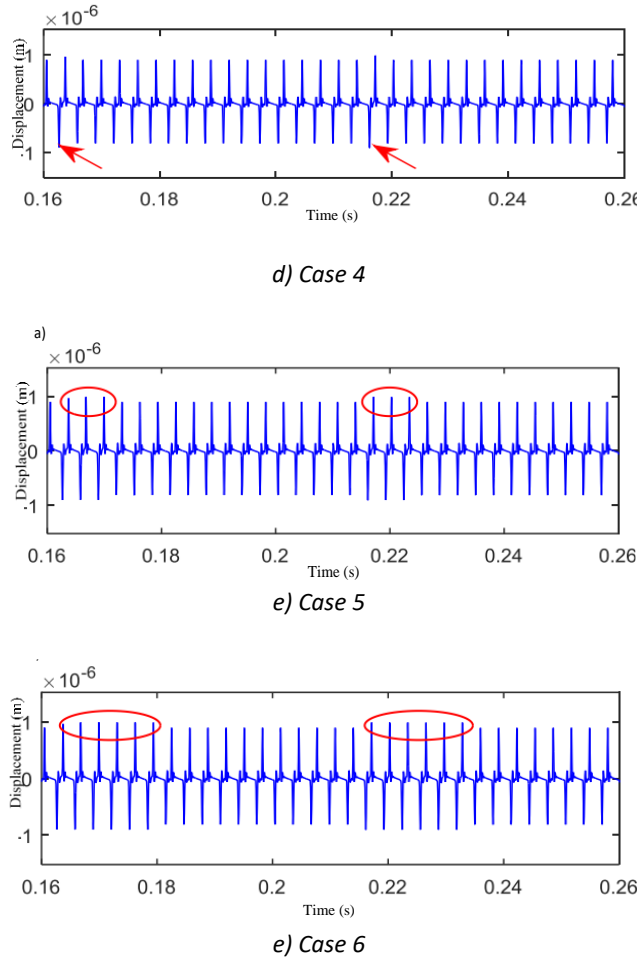

b) Case 2

c) Case 3

d) Case 4

e) Case 5

e) Case 6
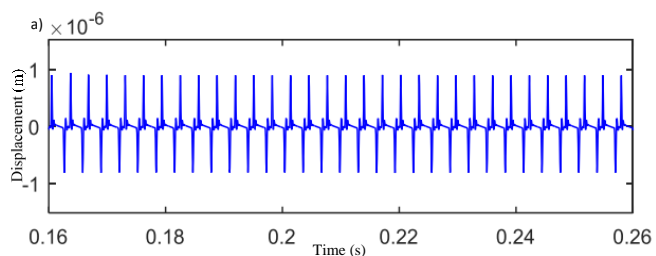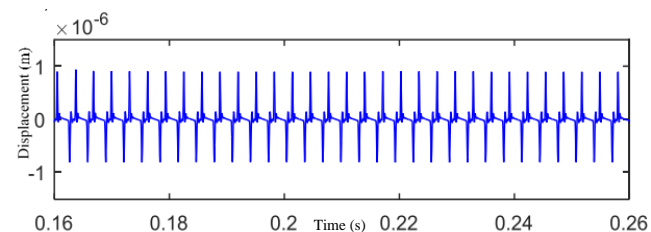
Fig. 4 Computed displacement of the pinion for faulty pinion cases.

Figure 4 gives z-direction displacement signals of the pinion for defect types descending from slight pitting to severe pitting, respectively. For defect type No. 1, as the field observations provided in Table 1 depict, the defective area is very small, and the consequent fault symptoms in Fig. 4 (a) are very weak. However, careful observation in Fig. 4(d) to (e) displays one or multiple spikes (circled and pointed by arrows) slightly bigger than others. Fig. 4(a) displays the displacement described above for pitting case No. 1, which is the main cause for generating the spike (1 pit, pitted area 0.5%). The small differences between the peak's amplitudes are reasonable because of the heavy masses of the gears. With this explanation, the time domain signals are not suitable and precise for fault detection. Thus, other procedures are needed for detecting defects in such circumstances, such as using some statistical specifics. Consequently, for validation purposes, some selected statistical features are calculated for the measured signals.

4.3 Tracing the failure using statistical features

As depicted in the previous section, defining the level of pitting in different cases cannot be accomplished by merely interpreting vibrational signals. Therefore, the research continued by estimating some statistical features to present the behavior of the selected cases. To this end, the statistical indicators of vibrational signals are calculated for the faulty cases and compared with their healthy states. It is helpful to comprehend how the different levels of pitting growth affect the conforming statistical parameters. The following equation is used to understand the change in statistical index.

$$Growth\ rate = \frac{F_i - F_0}{F_0} * 100\% \qquad (13)$$

F_0 stands for the statistical parameter of a healthy state, and F_i shows the ith failure. The thirty statistical features that are frequently used in most research are calculated for the displacement signals[34]. Then due to the sensitivity of these features and how they change during fault growth, it was decided which one showed the most sensitivity. Table 4 represents the formula for the selected statistical features.

Table 4 Representation of the selected statistical indices [34].

Definition	Name
The maximum value in $x(n)$	Maximum value
The minimum value in $x(n)$	Minimum value
$\bar{x} = \dfrac{1}{N}\sum_{n=1}^{N} x(n)$	Mean
$\dfrac{\max(x(n))}{\sqrt{\frac{1}{N}\sum_{n=1}^{N} x(n)^2}}$	Crest factor
$\dfrac{\max(x(n))}{\frac{1}{N}\sum_{n=1}^{N} x(n)^2}$	Clearance factor
$\dfrac{\frac{1}{N}\sum_{n=1}^{N}(d(n)-\bar{d})^6}{\left(\frac{1}{N}\sum_{n=1}^{N}(d(n)-\bar{d})^2\right)^3}$	M6A
$\dfrac{\frac{1}{N}\sum_{n=1}^{N}(d(n)-\bar{d})^8}{\left(\frac{1}{N}\sum_{n=1}^{N}(d(n)-\bar{d})^2\right)^2}$	M8A

In Table 4, the raw signal and the difference signal are presented with $x(n)$ and $d(n)$, respectively. The bar sign represents averaging.

The changes in statistical parameters of faulty cases in the time and frequency domains are presented in Figs. 5 and 6. According to the dimensions of the pits and teeth, the indices that could demonstrate these changes with the most sensitivity are selected.
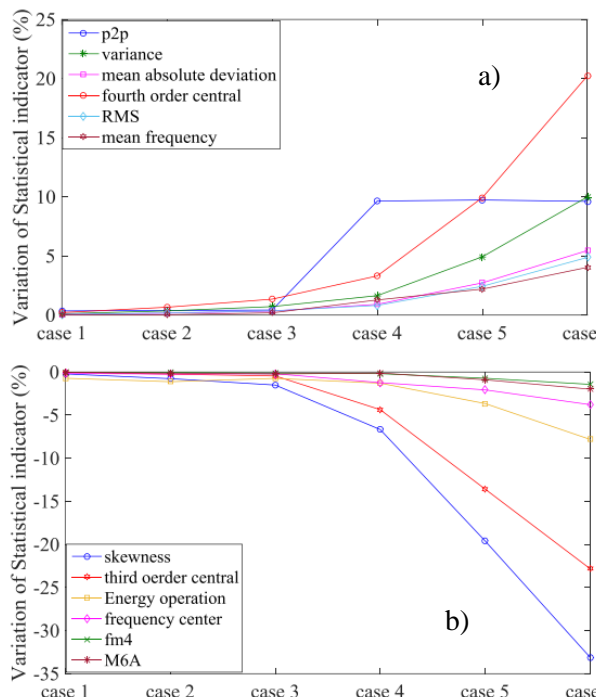

Fig. 5 Change of statistical features for different cases in the time domain.

As displayed in Fig. 5 (a), the growth rate for the selected statistical indexes steadily increased. Cases 1 and 2 are hardly distinguishable due to the tiny amount of removed surface. From cases 3 to 6, the differences in the estimated parameters are apparent. The fourth-order central moment and variance with 20% and 10% changes for case 6 exhibit the highest and second-highest sensitivity, respectively. It should be noted that variations of some indicators in the time domain (see Fig. 5 (b)) versus increasing severity of the defect types have negative slopes. The behavior of the statistical parameters that have steadily declined is also presented. The statistical indicator skewness with a -30% variation exposed the most sensitivity in the failure of case number 6. Among these indicators, fourth-order

central moment and skewness have the best capability for pitting fault detection in the time domain.
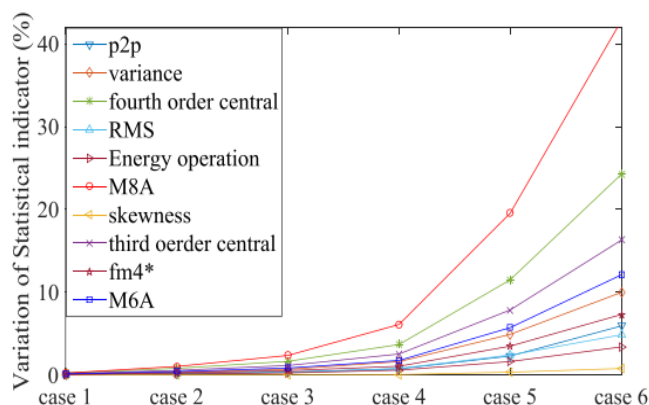

Fig. 6 Change of statistical parameters for different cases in the frequency domain.

In Fig. 6, the variation of statistical parameters in the frequency domain is presented. It is observed that the amplitudes of the parameters will increase gradually as the pitted area propagates in the pitted tooth (defect types become more severe). The statistical parameter variations are clearer in the frequency domain, especially M8A and fourth-order central moment, for fault detection.

5. Experimental setup

To evaluate the vibrational behavior of faulty gear cases, an experimental setup is prepared, Fig. 7. This setup is arranged with a 1:5 scale to a standard-sized gearbox. With the use of this rig, it is intended to examine the sensitivity of the selected statistical features that are used for gear fault identification.

The test setup consists of a pair of gears, an electric motor with 2.2 KW of power, and a braking system consisting of a spring and rope. This rig is prepared to build a scaled model of the original system. The electric motor drives the shaft and the pinion so that the power is delivered to the gear and the follower shaft. The braking system has a spring and a rope designed to apply torque to the follower shaft. For measuring the shaft speed, a tachometer is used.

For measuring the vibrational signals at the bearing support near the pinion, an accelerometer (CA-YD-189) with a sensitivity of 1000 mv/g was used. Then the measured signals were stored in a data logger of type Avant-7016. The pinion speed at this test is the

same as the theoretical calculations (18.7 Hz). Due to the described braking system that was explained before and the scaling factor of the test rig, a resisting torque of 14 Nm was applied through the rope and spring system to the follower shaft.
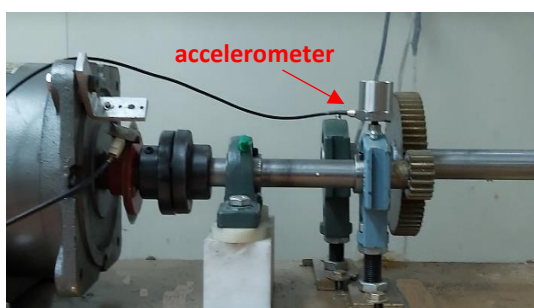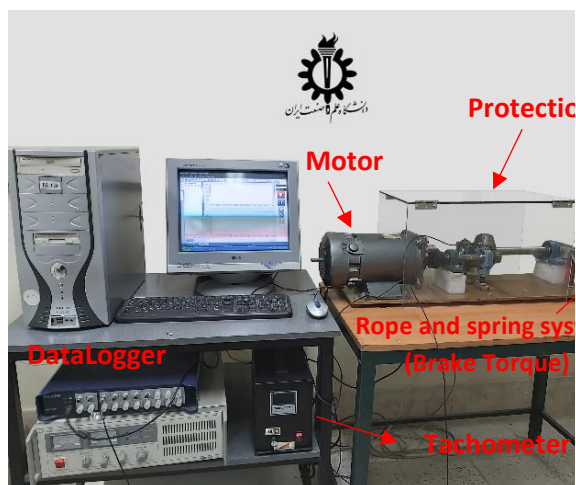
while the scale of actual pitting is preserved, Fig. 8.

Case 1   Case 2

Case 4   Case 5

Fig. 8. Faulty gears used for the test rig.

Fig. 7 The experimental test rig – a scaled model of a standard locomotive power transmission system gear with a 1:5 ratio.

Regarding the material content of the gears in the locomotive power transmission system, the experimental test rig is built with the same type of steel, which is VCN200.

As displayed in Fig. 7, for the measurement of the vibrational signals, an accelerometer is placed on the bearing in the vicinity of the pinion. The sampling frequency is 6 kHz. For different levels of fault growth that were explained before, the vibrational signals were collected. To model the different faulty cases with regard to the pitting growth, multiple holes in circular shapes are drilled on the tooth surface,
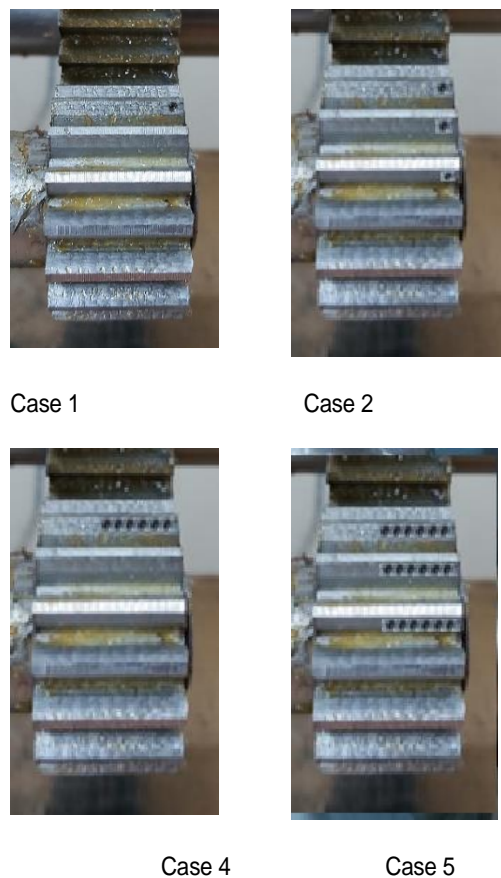
The power is transmitted through a shaft that connects the pinion and the electric motor. The initial tests are performed with a healthy pinion. This is followed by installing the faulty gears and taking several measurements.

The designated statistical features for all measurements are calculated in both the time and frequency domains. The pitting growth in different cases is assessed and compared.

The statistical indexes for each case are obtained. The difference between such features for healthy and defective gears is defined as the growth rate.

The statistical indices that present the best performance in fault identification (the larger change in relation to the different fault scenarios) are compared with the test results. The compatibility between the estimated and

measured results indicated the ability to identify the damaged gears through measurements.

The accuracy of the accelerometer that is used for the measurements is 1000 mv/g, and due to the measured signals, there is no harmful interference between the recorded signal and the accelerometer sensitivity.
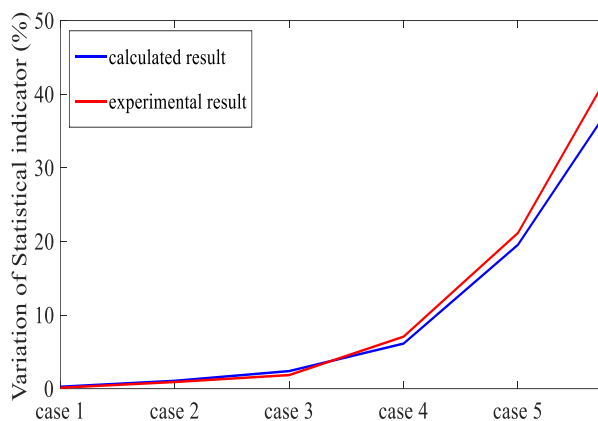

Fig. 9 Variations in M8A for the experimental setup.

6. Conclusion

This research presented an analytical model to calculate the effects of pitting growth in the gear power transmission system of locomotives. Time-dependent mesh stiffness for a healthy gear and six cases of pitting were evaluated. Correspondingly, the vibrational response of these six cases was analyzed. In the first three cases, only one pit in genuine dimensions was examined on one, three, and six teeth, respectively. Due to the geometry of the gear, variations in the vibration response were small. Then, to display growth in the pitted section, six pits were examined on one, three, and six teeth. Changes in the displacement signals were well observed. Finally, an experimental setup was prepared to validate the estimations for the selected statistical features. Through the calculation of the statistical indicators in the time and frequency domains, the following results were obtained:

- For most of the statistical identifiers, that is, cases 1 and 2, the change in statistical indicators is less than 2 percent, so the defects are hardly identifiable due to the small level of the

removed surface compared to pinion geometry.

- As the defect takes place on several teeth concurrently, like in case 3 with one pit on six teeth, the variation of M8a growth is about 2 folds, and it can be easily detected in the frequency domains.

- The variations in the statistical parameters in the time domain with respect to the damage propagation are categorized into two groups: the ones with a positive slope, among which the fourth-order central moment displays the most sensitivity with a 20 percent change between different scenarios, and the ones with a negative slope, in which skewness displays the most sensitivity with a 34 percent change.

- In the frequency domain, the growth in statistical parameters is observed to have a positive slope and value. Among these, M8A, with a 42 percent change, shows the most sensitivity.

- In the frequency domain, variations of statistical parameters were more apparent than in the time domain, and the propagations of damage were responded to with more uniform behavior. Thus, utilizing the statistical parameters in the frequency domain is a better pitting detection method.

The result for the experimental setup demonstrates that M8A displays an acceptable agreement with the theoretical result.

References

[1] Z. Chen, W. Zhai, and K. Wang, Dynamic investigation of a locomotive with effect of gear transmissions under tractive conditions. Journal of Sound and Vibration, 408 (2017) 220-233.

[2] F. Chaari, W. Baccar, M. S. Abbes, and M. Haddar, Effect of spalling or tooth breakage on gear mesh stiffness and dynamic response of a one-stage spur gear transmission. European Journal of Mechanics-A/Solids, 27(4) (2008) 691-705.

[3] L. Gelman, R. Zimroz, J. Birkel, H. Leigh-Firbank, D. M. Simms, B. Waterland, and G. Whitehurst, Adaptive

vibration condition monitoring technology for local tooth damage in gearboxes. (2005).

[4] Z. Chen, W. Zhai, and K. Wang, A locomotive–track coupled vertical dynamics model with gear transmissions. Vehicle System Dynamics, 55(2) (2017) 244-267.

[5] W. Bartelmus, Mathematical modelling and computer simulations as an aid to gearbox diagnostics. Mechanical Systems and Signal Processing,15(5) (2001) p. 855-871.

[6] F. Li, Y. Qin, L. Ge, Z. Pang, S. Liu, and D. Lin, Influences of planetary gear parameters on the dynamic characteristics–a review. Journal of Vibroengineering, 17(2) (2015) 574-586.

[7] Z. Chen and Y. Shao, Mesh stiffness calculation of a spur gear pair with tooth profile modification and tooth root crack. Mechanism and Machine Theory, 62 (2013) 63-74.

[8] Z. Chen, and Y. Shao, Dynamic simulation of spur gear with tooth root crack propagating along tooth width and crack depth. Engineering Failure Analysis. 18(8) (2011) p. 2149-2164.

[9] I. Howard, S. Jia, and J. Wang., The dynamic modelling of a spur gear in mesh including friction and a crack. Mechanical systems and signal processing. 15(5) (2001) p. 831-853.

[10] S. Wu, M. J. Zuo and A. Parey, Simulation of spur gear dynamics and estimation of fault growth. Journal of Sound and Vibration, 317(3-5) (2008) p. 608-624.

[11] Z. Feng, and M.J. Zuo, Vibration signal models for fault diagnosis of planetary gearboxes. Journal of Sound and Vibration, 331(22): (2012) p. 4919-4939.

[12] H. Henao, S.H. Kia, G.A. Capolino, Torsional-vibration assessment and gear-fault diagnosis in railway traction system, IEEE Trans. Indust. Electron. (2011) 58

[13] C. Zhe, H. Niaoqing, G. Fengshou and Q. Guojun, Pitting damage levels estimation for planetary gear sets based on model simulation and grey relational analysis. Transactions of the Canadian Society for Mechanical Engineering, 35(3) (2011) 403-417.

[14] S. A. Abouel-seoud, E. S. Dyab and M. S. Elmorsy, Influence of tooth pitting and cracking on gear meshing stiffness and dynamic response of wind turbine gearbox. Int. J. Sci. Adv. Technol, 2(3) (2012) 151-165.

[15] F. Chaari, T. Fakhfakh and M. Haddar, Dynamic analysis of a planetary gear failure caused by tooth pitting and cracking. Journal of Failure Analysis and Prevention, (6) 2 (2006) 73-78.

[16] F.K. Choy, V. Polyshchuk, J.J. Zakrajsek., Analysis of the effects of surface pitting and wear on the vibration of a gear transmission system. Tribology international, 29(1): (1996) p. 77-83.

[17] L. Liu, X. Liang, and M.j. Zuo, Vibration signal modeling of a planetary gear set with transmission path effect analysis. Measurement, (2016) 85, 20-31.

[18] X. Liang, M.J. Zuo, and T.H Patel, Evaluating the time-varying mesh stiffness of a planetary gear set using the potential energy method. Proceedings of the Institution of Mechanical Engineers, Part C: Journal of Mechanical Engineering Science, 228(3), (2014) 535-547.

[19] X. Tian, M.J. Zuo and K.R. Fyfe. Analysis of the vibration response of a gearbox with gear tooth faults. in ASME 2004 International Mechanical Engineering Congress and Exposition. American Society of Mechanical Engineers. (2004)

[20] A.F. Rincon, F. Viadero, M. Iglesias, A. de-Juan, P. Garcia, R. Sancibrian, Effect of cracks and pitting defects on gear meshing. Proceedings of the Institution of Mechanical Engineers, Part C: Journal of Mechanical Engineering Science, 226(11), (2012), 2805-2815.

[21] H. Ma, Z. Li, M. Feng, R. Feng, and B. Wen, Time-varying mesh stiffness calculation of spur gears with spalling defect. Engineering Failure Analysis, 66, (2016) 166-176.

[22] A. Saxena, A. Parey, and M. Chouksey, Time varying mesh stiffness calculation of spur gear pair considering sliding friction and spalling defects. Engineering Failure Analysis, 70, (2016) 200-211.

[23] M. Rezaei, M. Poursina, S.H. Jazi and F.H. Aboutalebi, Multi crack detection in helical gear teeth using transmission error ratio. Journal of Mechanical Science and Technology, 33(3), (2019) 1115-1121.

[24]   X. Liang, H. Zhang, L. Liu and M. J. Zuo, The influence of tooth pitting on the mesh stiffness of a pair of external spur gears. Mechanism and Machine Theory, (2016),106, 1-15.

[25]   J. Hou, S. Yang, Q. Li, Y. Liu, Effect of a novel tooth pitting model on mesh stiffness and vibration response of spur Gear. Mathematical Method and Application of machine learning. (2022)

[26]   SG. Thunuguntla, A. Hood, C. Cooley, "Tooth Mesh Characterization Of Spur Gear Pairs With Surface Pitting Damage," SAE Technical Paper (2023)

[27]   M. Grzeszkowski, S. Nowoisky, P. Scholzen, G. Kappmeyer, C. Gühmann, J. Brimmers, and C. Brecher. "Classification of gear pitting damage using vibration measurements." tm-Technisches Messen 88, no. 5 (2021): 282-293.

[28]   Happi, Kemajou Herbert Yakeu, Bernard Xavier Tchomeni Kouejou, and Alfayo Anyika Alugongo. "Influence of Coexistence of Pitting and Cracking Faults on a Two-Stage Spur Gear System." Vibration 6.1 (2023): 195-217.

[29]   Ren, Yulin, Guoyan Li, Xiong Li, Jingbin Zhang, Runjun Liu, and Sifan Shi. "Compound Fault Characteristic Analysis for Fault Diagnosis of a Planetary Gear Train." Sensors 24, no. 3 (2024): 927.

[30]   Kong, Yiyi, Hong Jiang, Ning Dong, Jun Shang, Pengfei Yu, Jun Li, Manhua Yu, and Lan Chen. "Analysis of Time-Varying Mesh Stiffness and Dynamic Response of Gear Transmission System with Pitting and Cracking Coupling Faults." *Machines* 11, no. 4 (2023): 500.

[31]   F. Niksai, M.A. Rezvani. Concurrent impact of chipping and pitting damages in a locomotive power transmission system. J Mech Sci Technol 36, (2022) 3791-3800.

[32]   T. Ouyang, G. Wang, L. Cheng, J. Wang "Comprehensive diagnosis and analysis of spur gears with pitting-crack coupling faults." Mechanism and Machine Theory 176 (2022): 104968.

[33]   X. Liang, M. J. Zuo and Z. Feng, Dynamic modeling of gearbox faults: A review. Mechanical Systems and Signal Processing, 98, (2018) 852-876.

[34]   X. Zhao, M. J. Zuo and Z. Liu, Diagnosis of pitting damage levels of planet gears based on ordinal ranking. In 2011 IEEE Conference on Prognostics and Health Management (pp. 1-8). IEEE. (2011, June).

[35]   Z. Liu, J. Qu, M. J. Zuo and H. B. Xu, Fault level diagnosis for planetary gearboxes using hybrid kernel feature selection and kernel Fisher discriminant analysis. The International Journal of Advanced Manufacturing Technology, 67(5-8) (2013)1217-1230.

[36]   X. Zhao, M. J. Zuo, Z. Liu and M. R. Hoseini, Diagnosis of artificially created surface damage levels of planet gear teeth using ordinal ranking. Measurement, 46(1), (2013) 132-144.

[37]   X. Liang, Z. Liu, J. Pan, M. Zuo, Spur gear tooth pitting propagation assessment using model-based analysis. Chinese Journal of Mechanical Engineering 30.6 (2017): 1369-1382.

[38]   D.C.H. Yang and Z.S. Sun, "A Rotary Model for Spur Gear Dynamics," ASME Journal of Mechanisms, Transmissions, and Automation in Design, 107, PP. 529-535, 1985.

[39]   M. Amabili and A. Rivola, Dynamic analysis of spur gear pairs: steady-state response and stability of the SDOF model with time-varying meshing damping. Mechanical systems and signal processing, 11(3), (1997), 375-390.